Available online at www.sciencedirect.com

SciVerse ScienceDirect

journal homepage: www.elsevier.com/locate/he

Nanosized Pt/IrO_2 electrocatalyst prepared by modified polyol method for application as dual function oxygen electrode in unitized regenerative fuel cells

J.C. Cruz [a], V. Baglio [b], S. Siracusano [b], R. Ornelas [c], L.G. Arriaga [a], V. Antonucci [b], A.S. Aricò [b,*]

[a] Centro de Investigación y Desarrollo Tecnológico en Electroquímica S.C., Parque Tecnológico Querétaro, Sanfandila, Pedro Escobedo, Querétaro, México

[b] CNR-ITAE, Via Salita S. Lucia sopra Contesse 5, 98126 Messina, Italy

[c] Tozzi Renewable Energy SpA, Via Zuccherificio, 10-48010 Mezzano (RA), Italy

ARTICLE INFO

Article history:
Received 20 October 2011
Received in revised form
21 December 2011
Accepted 28 December 2011
Available online 23 January 2012

Keywords:
URFC
Pt/IrO_2
Water electrolysis
Fuel cell
Polyol method

ABSTRACT

A new generation of highly efficient and non-polluting energy conversion and storage systems is vital to meeting the challenges of global warming and the finite reality of fossil fuels. In this work, nanosized Pt/IrO_2 electrocatalysts are synthesized and investigated for the oxygen evolution and reduction reactions in unitized regenerative fuel cells (URFCs). The catalysts are prepared by decorating Pt nanoparticles (2–10 nm) onto the surface of a nanophase IrO_2 (7 nm) support using an ultrasonic polyol method. The synthesis procedure allows deposition of metallic Pt nanoparticles on Ir-oxide without causing any occurrence of metallic Ir. The latter is significantly less active for oxygen evolution than the corresponding oxide. This process represents an important progress with respect to the state of the art in this field being the oxygen electrocatalyst generally obtained by mechanical mixing of Pt and IrO_2. The nanosized Pt/IrO_2 (50:50 wt.%) is sprayed onto a Nafion 115 membrane and used as dual function oxygen electrode, whereas 30 wt.% Pt/C is used as dual function hydrogen electrode in the URFC. Electrochemical activity of the membrane-electrode assembly (MEA) is investigated in a single cell at room temperature and atmospheric pressure both under electrolysis and fuel cell mode to assess the perspectives of the URFC to operate as energy storage device in conjunction with renewable power sources.

1. Introduction

Hydrogen energy storage systems coupled to renewable power sources are being proposed as a means to increase energy independence, improve domestic economies, and reduce greenhouse gas emissions from stationary and mobile fossil-fueled sources [1–3]. New technologies for production and utilization of hydrogen as energy carrier include electrolysers [4–6] and fuel cells [7–9], respectively. Both processes may alternatively occur in the same device based on a proton exchange membrane (PEM). This device is called unitized regenerative fuel cell (URFC). Compared with conventional

* *Corresponding author*. Tel.: +39 (0)90 624237; fax: +39 (0)90 624247.
E-mail address: arico@itae.cnr.it (A.S. Aricò).

0360-3199/$ – see front matter
doi:10.1016/j.ijhydene.2011.12.153

secondary batteries, URFCs advantages rely on high energy density, long-term energy storage, durability and environmental protection [10–13]. Whereas in comparison to the separate fuel cell and electrolyzer based systems, URFCs are significantly more compact and they allow considerable system simplification. URFC devices are characterized by rapid start up, they can operate efficiently at low temperature without the need of cumbersome power consuming auxiliaries. Moreover, they can provide stable operation even in the presence of a large number of start up/shut down cycles.

Nevertheless, the design of an oxygen electrode for an electrolyser is different than that of a fuel cell [14]. Carbon supported Pt electrocatalysts, currently used in fuel cells, are characterized by low catalytic activity and poor stability for oxygen evolution [15]. It is important to consider that the present Pt/C catalysts do not yet satisfy completely the stability requirements of a fuel cell cathode characterized by an operating potential window of 0.6–1.0 V vs RHE [16], whereas that of an oxygen evolution electrode, in an electrolyzer, is normally 1.5–2.0 V vs RHE [17,18]. Moreover, for the oxygen electrode in a polymer electrolyte fuel cell, the gas diffusion layer (GDL) is usually a highly hydrophobized carbon paper or carbon cloth [16]. However, this type of GDL cannot be used in an URFC mainly for the following two reasons: (i) the carbon material easily oxidizes to CO_2 at high potentials during water electrolysis causing poor stability, and (ii) GDLs must be characterized by an appropriate balance between hydrophobic and hydrophilic properties for both fuel cell and water electrolysis operation modes to promote mass transport of the reaction species to the catalytic sites and removal of reaction products [17]. While the electrode for a water electrolyser is generally designed to be flooded or partially flooded [17], the fuel cell operating at low temperatures must repel water to avoid electrode flooding thus allowing access of molecular H_2 and O_2 to the catalytic sites [16]. From such an analysis, it is clear that the URFC is not the simple linear combination of electrodes used in fuel cells with those used in electrolysis cells.

Beside these aspects, one of the main technical breakthroughs for URFCs is the development of efficient dual function electrocatalysts for the oxygen reaction [19–25]. Nanostructured electrocatalysts are attracting a deal of interest in this field since they have a strong impact on the dispersion of precious metals and the possibility of tailoring electrochemical properties due to the relevant influence of the surface characteristics on the overall behavior [1,26]. The materials for dual function oxygen electrodes actually include Pt–Ir [27,28], Pt-Ru-Ir [29], Pt-IrO_2 [30–34], Pt-IrO_2-RuO_2 [21,35]. Various methods have been used to prepare the separate catalytic IrO_2 and Pt phases forming the dual function electrocatalyst, i.e. Adams fusion, sol–gel, etc [36–38]. However, the final step is characterized in most cases by a mechanical grinding and mixing of the catalyst powders to form the dual function electrode [21]. It is considered that even extensive ball milling procedures can hardly allow to achieve a good mixing at an atomic level of the two phases to provide a suitable catalytic dispersion. Alternatively, the direct (one step) chemical synthesis of dual function catalyst is not a simple task. One critical aspect is regarding the achievement of nanosized metallic platinum nanoparticles in combination with a dispersed Ir-oxide phase. The occurrence of metallic Ir or a substoichiometric Ir-oxide phase during the Pt precursor reduction step to form Pt° may cause a decrease of electrocatalytic activity for water electrolysis [21,39]. The polyol process has recently received attention for preparation of fuel cell catalysts [40,41] because it provides a satisfactory control of Pt particle size and distribution without using any additional stabilizer [42–45]. By using ethylene glycol in the polyol process, metal ions are reduced to form a metal colloid; they receive electrons from the oxidation of ethylene glycol to glycolic acid, which is present in its deprotonated form as glycolate anions [46].

The novelty of the present approach consists in the use of modified polyol process to form Pt nanoparticles directly on a high surface area IrO_2 support by proper control of the reducing process. Formation of a metallic Pt on IrO_2 thus occurs without significant modification of the oxidation state of Ir. Accordingly, IrO_2-nanophase supported Pt nanoparticles were prepared by using an ultrasonic polyol method in order to obtain an efficient dual function catalyst for oxygen reduction (Pt) [45,47] and evolution (IrO_2) [48–50]. Characterization of catalysts was carried out by X-ray diffraction (XRD), X-ray fluorescence (XRF), X-ray photoelectron spectroscopy (XPS) and transmission electron microscopy (TEM). It was studied the effect of Pt nanoparticles growth as a function of the pH of reaction and the reaction yield. The URFC processes were studied at room temperature and atmospheric pressure to assess their perspectives to operate as energy storage devices in combination with renewable power sources.

2. Experimental

2.1. *Preparation of Pt/IrO_2 electrocatalysts*

IrO_2 nanoparticles were prepared by using a low temperature colloidal method [50]. In order to obtain a dual function catalyst consisting of Pt supported on IrO_2 nanoparticles, the ultrasonic polyol method, commonly used to prepare Pt or other elements in a metallic form on a carbon support [51–55], was employed. 25 mL of ethylene glycol (Aldrich 99%) were placed in a beaker; this was kept in an ultrasonic bath for 10 min at ~70 °C. Afterwards, 50 mg of in-house prepared IrO_2 were added in the beaker and this solution was maintained under ultrasounds (frequency 40 kHz) at 70 °C for 10 min. Then, 1 mL of 0.5 M H_2PtCl_6 (22.75 wt.% of Pt, Engelhard) was added and reaction time was varied, with periods of 10, 30 and 60 min. The final solution was centrifuged for 30 min and filtered to separate liquid and solid phases. During the polyol synthesis process, the pH of the solution was varied in order to modulate the reducing power of ethylene glycol and thus the reaction rate. The effect of this parameter in determining the crystallite size of Pt was investigated. A scheme of the Pt-IrO_2 electrocatalyst preparation procedure is reported in Fig. 1.

2.2. *Physico-chemical characterization*

X-ray diffraction powder (XRD) patterns for these catalysts were obtained on a Philips X'Pert X-ray diffractometer using Cu Kα-source operating at 40 kV and 30 mA. The diffraction

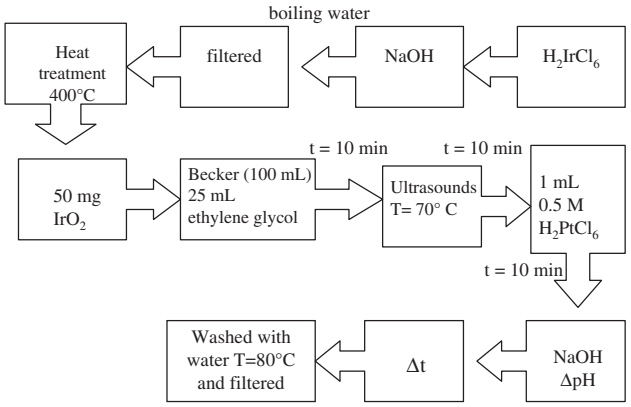

Fig. 1 – Polyol ultrasonic synthesis process for obtaining Pt nanoparticles on IrO_2 support.

patterns were fitted to JCPDS (Joint Committee on Powder Diffraction Standards) and crystallite size distribution was calculated using LBA (line broadening analysis) [16]. X-ray fluorescence analysis of the catalysts was carried out by a Bruker AXS S4 Explorer spectrometer operating at a power of 1 kW and equipped with a Rh X-ray source, a LiF220 crystal analyser and a 0.12° divergence collimator.

The morphology of catalysts was investigated by transmission electron microscopy (TEM) using a Philips CM12 instrument. Specimens were prepared by ultrasonic dispersion of the catalysts in isopropyl alcohol and thereafter by depositing a drop of suspension on a carbon-coated grid.

2.3. *Preparation of membrane and electrode assembly (MEA)*

A Nafion 115 (Ion Power) membrane was used as the solid polymer electrolyte. The oxygen reduction/evolution catalyst was directly deposited onto one side of the membrane by a hot-spray technique. Inks were composed of aqueous dispersions of catalyst, deionised water, Nafion® solution (5% Aldrich) and anhydrous ethanol (Carlo Erba, Italy); the Pt/IrO_2 (50:50 wt.%) catalyst loading was 0.5 mg cm^{-2}. A commercial 30% Pt/Vulcan XC-72 (E-TEK, PEMEAS, Boston, USA) was used as catalyst for the dual function hydrogen electrode. The hydrogen electrode catalyst ink was prepared by directly mixing in an ultrasonic bath a suspension of Nafion ionomer in water with a Pt/C catalyst powder [56]. The obtained paste was spread on a carbon cloth backing (GDL ELAT from E-TEK) to obtain a Pt loading of 0.3 mg cm^{-2}. The ionomer content in both electrodes was 33 wt.% in the catalytic layer after drying. The geometrical area of the electrode was 5 cm^2. The MEA was directly installed in the cell housing and compresed by tightening at 9 N•m using a dynamometric wrench. A Ti grid (Franco Corradi, Italy) backing layer was used at the oxygen compartment [57–59].

2.4. *Electrochemical characterization of the MEA*

The URFC electrochemical behaviour was evaluated by electrochemical impedance spectroscopy (EIS) in a frequency range 10 kHz–10 mHz and steady-state voltammetry by using potentiostatic control in a potential window from 0 to 1.8 V. The electrochemical characterization was performed by a PGSTAT Autolab 302 potentiostat/galvanostat equipped with a booster of 20 A (Metrohm) and a Frequency Response Analyser (FRA). A fuel cell test station typically employed for operation with both hydrogen and liquid fuels (Fuel Cell Tech., Inc.) was used in the present case to control operating parameters, such as gases and liquid water flow rate, etc. The electrolyser performance was evaluated at room temperature. Deionised water was circulated by a pump at a flow rate of 2 ml min^{-1}; it was supplied to the oxygen electrode compartment at atmospheric pressure. The fuel cell performance was carried out under atmospheric pressure at room temperature by feeding dry H_2 and air at a flow rate of 50–150 scc min^{-1}, respectively.

3. Results and discussion

The structural characteristics of the 30% Pt/C catalyst for the hydrogen evolution/reduction reactions were already reported in a previous paper [60]. In the present work, we have focused the attention on the oxygen reduction/evolution catalysts. Fig. 2 shows the XRD patterns of the IrO_2 support synthesized by the colloidal method and Pt/IrO_2 catalysts obtained at different pH values varying from 3 to 11.7 by using the ultrasonic polyol method (10 min). The XRD peaks were

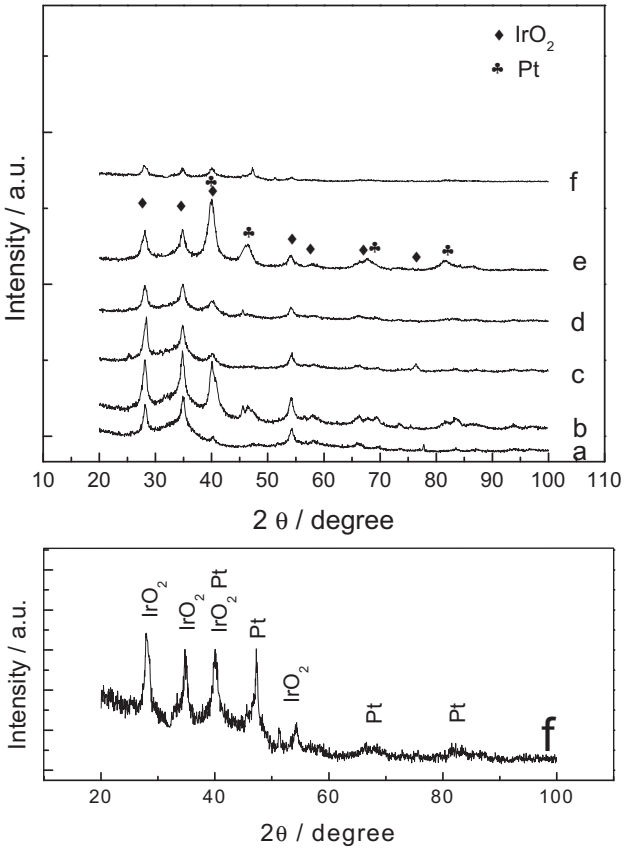

Fig. 2 – Powder XRD patterns of IrO_2 in house (a) and Pt-IrO_2 at different pH values: (b) 3, (c) 5, (d) 9, (e) 10 and (f) 11.7.

assigned to IrO_2 tetragonal crystallographic structure and the face centered cubic (fcc) structure of metallic Pt. The mean crystallite size was estimated from the broadening of the main peaks by the Debye-Scherrer equation [16]. The crystallite size was found to be about 7 nm for IrO_2 and in the range of 2.7–10 nm for Pt as a function of the pH. Fig. 3 shows that there is a sigmoidal variation of Pt crystallite size as a function of pH for a fixed reaction time (10 min). This evidence was reported previously for PtRu catalysts [46] and it appears as a useful tool to tailor the Pt particle size within this preparation method. The reaction mechanism is shown to involve the oxidation of the solvent, ethylene glycol, to mainly glycolic acid or, depending on the pH, its anion, glycolate. Glycolate is believed to act as a good stabilizer for the colloids, possibly forming chelate-type complexes via its carboxyl groups [46]. Such interactions between the Pt catalysts and the neutral, acidic form, that is, glycolic acid, are smaller, and glycolic acid is believed to be a poor stabilizer. Therefore, the pH of the synthesis solution is expected to greatly influence the stability and size of the resulting colloids. It is well known in the literature concerning with Pt fuel cell catalysts that strong reducing agents, such as $NaBH_4$ in aqueous solutions, cause the occurrence of large Pt particles, whereas reduction in formic acid or hydrogen (diluted in nitrogen) at low temperature can allow formation of fine Pt particles [16,42,45,47]. Strong reducing agents are appropriate to form Pt alloys with non-noble transition metals which are less easily reduced than Pt [16,42,45,47]. However, in the present case, the objective is to avoid the reduction of Ir-oxide phase. Being Ir a noble metal with characteristics similar to Pt, generally, it is reduced in conjunction with Pt by most of the common reducing agent. The present procedure provides a tool to modulate the reducing power in the reaction environment in order to reduce selectively Pt, and with a convenient particle size. In the experiment reported in Fig. 3, the reaction time was maintained constant at 10 min. Yet, at high pH values, this reaction time is not sufficient to achieve a high reaction yield. In another experiment, the pH was fixed at 11.7 and the reaction time was varied. The reaction yield was monitored by comparing the catalyst experimental weight with the nominal one and determining the effective Pt and IrO_2 relative contents in the final catalyst using XRF. 50 wt.% Pt- 50 wt.% IrO_2 was the nominal content and 100% reaction yield was achieved when the experimental weight was equal to the nominal one. Fig. 4 shows the variation of Pt wt.% content in the catalyst with respect to reaction time at a temperature of ~70° C and pH 11.7 according to the results obtained by XRF. An increase of particle size of Pt from 2.7 to 5.5 nm was observed as the reaction time increased, and the Pt content was approaching the nominal one as well as the reaction yield reached about 100% (not shown). The increase of particle size during the reaction process is possibly due to the decrease of nucleation rate and occurrence of a particle growth mechanism with time. In other words, the preferred sequence for Pt precursor displacement appears to be in the order: metallic Pt particles of proper size (>2–3 nm), IrO_2 crystallites (7 nm), Pt nuclei (<2 nm). Since a crystallite size of 4–5 nm for Pt particles represents a good compromise in terms of activity and stability [16] in the potential window 0–2 V, we have selected the last preparation conditions to obtain the desired electrocatalyst characteristics. These specifically concern with a pH of reaction of 11.7 and a reaction time of 1 h to obtain 50:50 wt.% (Pt:IrO_2) with Pt crystalline size of 5.5 nm and IrO_2 crystalline size of 7 nm. Fig. 5 shows the XRD patterns of the selected Pt/IrO_2 catalyst with optimal characteristics; IrO_2 support is also reported for comparison.

Figure 6 shows a TEM analysis of this sample. A good dispersion of Pt clusters on the surface of IrO_2 agglomerates is clearly observed on the basis of the different atomic contrast as well as from the observation of lattice fringes especially those of the rutile tetragonal phase of IrO_2 (Fig. 6B). The dimension of Pt particles is in the range of 3–6.5 nm; whereas, IrO_2 particle size is in the range 5–9 nm. The morphology of the electrocatalyst appears as a decoration by Pt nanoparticles of the IrO_2 agglomerates. The size distribution analysis was obtained from a group of 300 counts made on several TEM

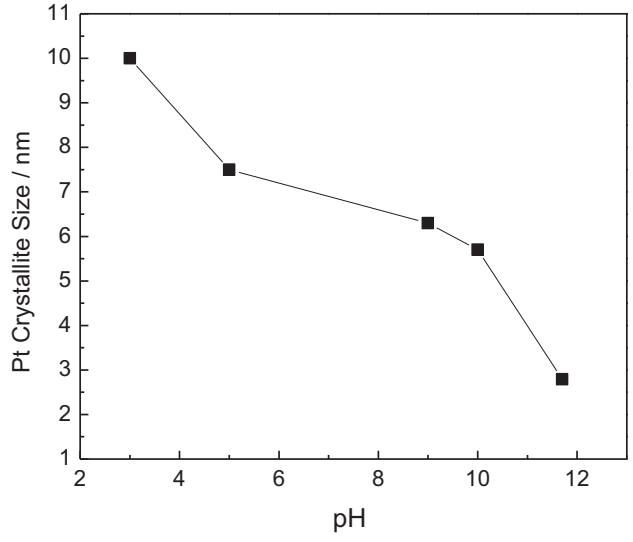

Fig. 3 – Variation of Pt crystallite size as a function of pH for a reaction time of 10 min.

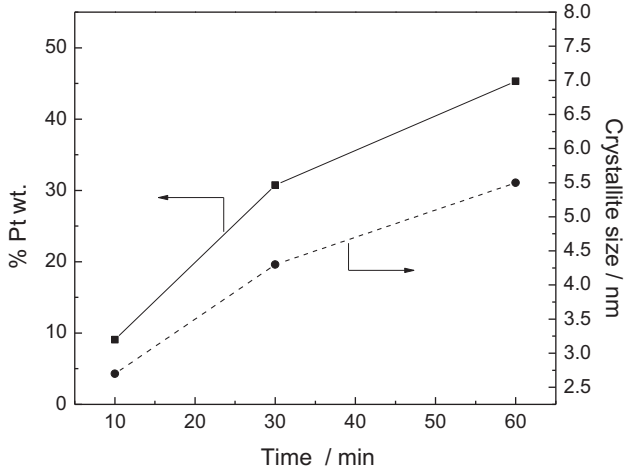

Fig. 4 – XRF variation of percent by weight of Pt with respect to time at T = 70° C and variation of crystallite size at pH 11.7.

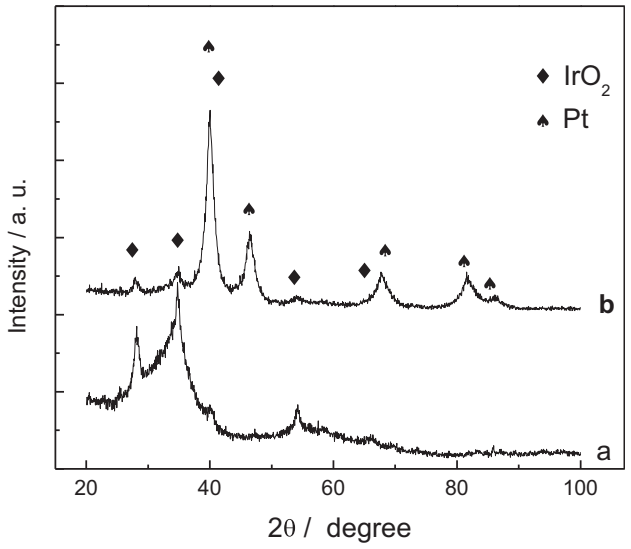

Fig. 5 – Powder XRD patterns of IrO_2 via colloidal process (a) and Pt-IrO_2 (~50:50 wt.%) via polyol ultrasonic process (b).

pictures which showed a mean size of about 5 nm for Pt (Fig. 6C and 7) nm for IrO_2 (Fig. 6D).

XRD and TEM analyses shown above have provided a clear indication that there is no occurrence of metallic Ir in the bulk and that the Ir is present as IrO_2 (rutile tetragonal phase). However, since electrochemical reactions occur at the catalyst–electrolyte interface, it is also important to investigate the catalyst surface properties. In fact, the outermost atomic layers may be more affected by the reduction process during catalyst preparation.

X-ray photoelectron spectroscopy was thus carried out on the selected Pt/IrO_2 electrocatalyst. A high resolution analysis of Pt 4f and Ir 4f regions (Fig. 7) reveals the prevailing occurrence of metallic Pt as well as oxidized Ir in the outermost catalyst layers. The presences of metallic Pt for the Pt $4f_{7/2}$ – Pt $4f_{5/2}$ doublet is clearly indicated by the fact that the Pt $4f_{7/2}$ peak is centered at 70.4 eV, whereas the Ir $4f_{7/2}$ – Ir $4f_{5/2}$ doublet appears more broadened with the Ir $4f_{7/2}$ peak occurring at 62.5 eV. This reflects the presence of both Ir^{3+} and Ir^{4+} oxidation states on the outermost atomic layers [61]. The value of binding energy for Ir $4f_{7/2}$ in the present electrocatalyst is essentially the same of a highly performing Ir-oxide catalysts used for oxygen evolution only [49,50]. XPS results provide an important indication that the present procedure allows to achieve a selective reduction of Pt to form metallic particles avoiding formation of metallic Ir even in the outermost atomic layers. This combination (Pt°-IrO_x) maximizes the catalytic activity for oxygen evolution/reduction [17,33].

The thermodynamic redox potential for the reduction of Pt-oxide to metallic Pt in acidic environment is 0.98 V vs. RHE whereas reduction of IrO_2 to metallic Ir is thermodynamically favored below 0.93 V vs. RHE [62]. Thus, there is just a small potential window in which the reduction of Pt-oxide may occur without causing reduction of IrO_2 to metallic Ir. In this regard, our results show that it is possible to achieve this goal by selecting mild reducing agents.

The optimized Pt/IrO_2 (50:50) electrocatalyst was investigated as oxygen electrode in a PEM URFC single cell operating at room temperature and atmospheric pressure. Electrochemical ac-impedance spectroscopy (EIS) was initially used to deconvolute ohmic characteristics from polarization behavior. Discrimination of the different contributions to the overall electrochemical behavior is made on the basis of the different relaxation times being the ohmic resistance

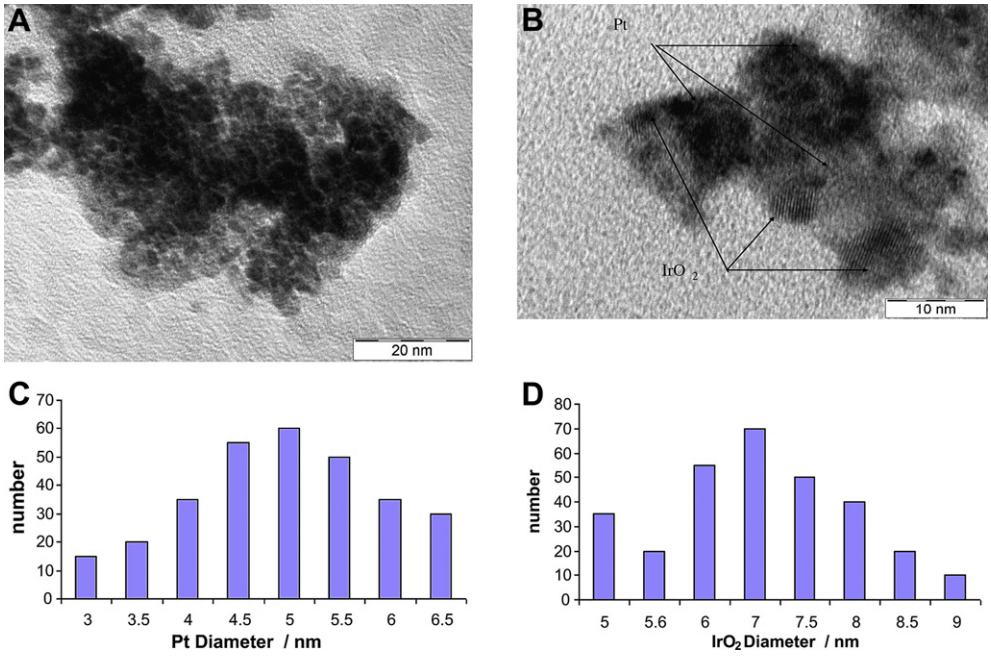

Fig. 6 – HR-TEM images of sample Pt-IrO_2 50:50 wt.% at different magnifications: (A) 330 kx, (B) 570 kx, (C) Particle size distribution for Pt and (D) Particle size distribution for IrO_2.

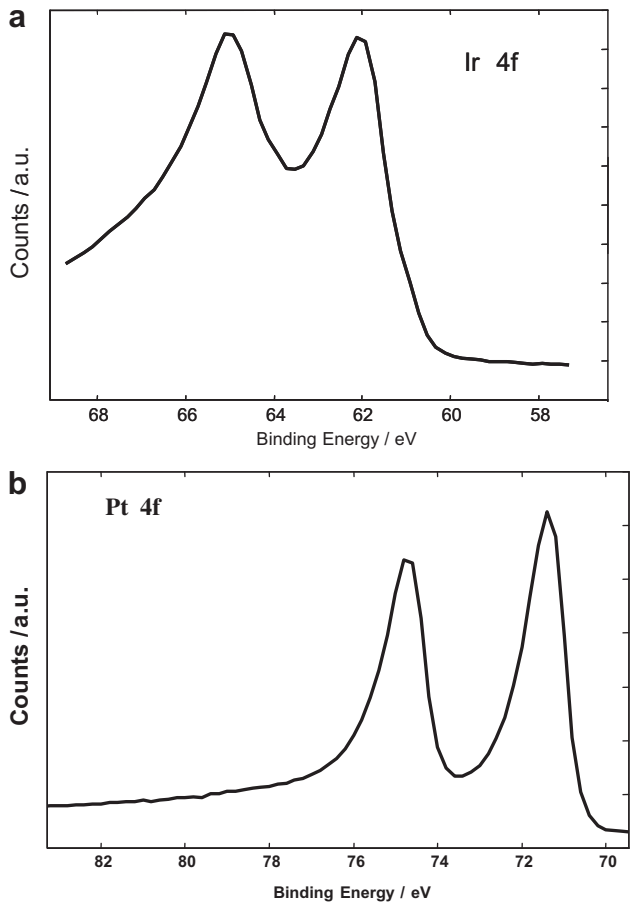

Fig. 7 – X-ray photoelectron spectra for the sample Pt/IrO_2: (A) Ir 4f and (B) Pt 4f.

characterized by high frequency response and polarization resistance by low frequency. Series and charge transfer resistances were thus evaluated by means of EIS at a terminal cell voltage of 1.5 V Fig. 8 shows the EIS spectrum of the URFC

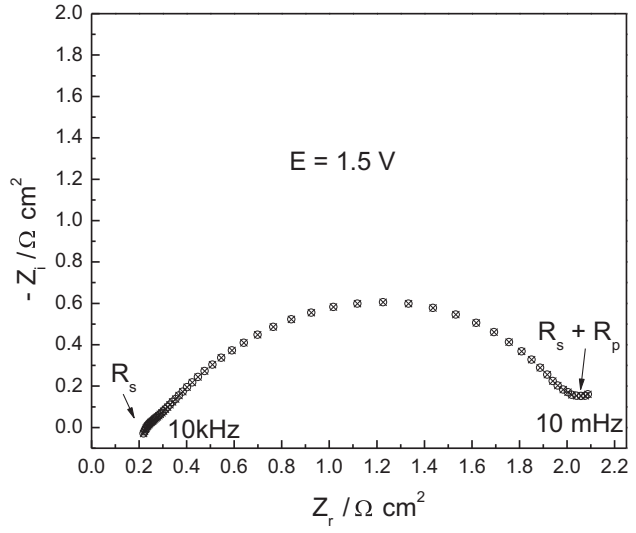

Fig. 8 – Impedance spectroscopy of a URFC in mode electrolyzer at room temperature and 1.5 V.

under electrolysis mode for the above mentioned Pt/IrO_2 catalyst at room temperature under atmospheric pressure. Under these conditions the oxygen reaction is the rate determining step and the hydrogen electrode can be assumed as reference electrode. The impedance plot (Nyquist) reveals a series resistance value of 0.23 Ω•cm^2; whereas, the polarization resistance was about 1.8 Ω•cm^2. The series resistance is mainly determined by the ohmic drop at the Nafion 115 solid polymer electrolyte (about 50%) but also by the contribution of contact resistances, electrode resistance and Ti-backing layer. However, at 1.5 V, which is very close to the thermoneutral potential of 1.48 V for water splitting, the polarization resistance is largely prevailing over the ohmic drop. This strongly indicates the need to enhance electrocatalytic properties [63].

The electrochemical behavior both in electrolysis and fuel cell mode is shown in Fig. 9. This performance is compared with that of a catalyst prepared by mechanical mixing of metallic Pt and IrO_2. The separate catalysts are prepared using the same procedures adopted for the dual-function catalyst. For what concerns the electrolysis, a maximum current density of 540 mA cm^{-2} at terminal cell voltage of 1.8 V, room temperature and atmospheric pressure, is achieved for both MEAs, since the same catalyst, i.e. IrO_2, acts for the oxygen evolution reaction, without any decrease of performance for the synthesized catalyst caused by the reduction process. Instead, the polarization curve obtained under fuel cell mode under the same operating conditions shows a limiting current density of 342 mA cm^{-2} for the in-house synthesized catalyst at room temperature, whereas a lower current density is recorded with the mixed catalyst probably due to a lower dispersion of this catalyst compared to synthesized one. The maximum power density obtained for the fuel cell based on the polyol-based dual function catalyst in these conditions (room temperature, atmospheric pressure) is slightly higher than 100 mW cm^{-2}. Although the fuel cell performance presently obtained at room temperature and ambient pressure may appear somewhat lower than that achieved in PEMFC devices for automotive applications operating at 80 °C and above [16,54], it is considered that such power densities

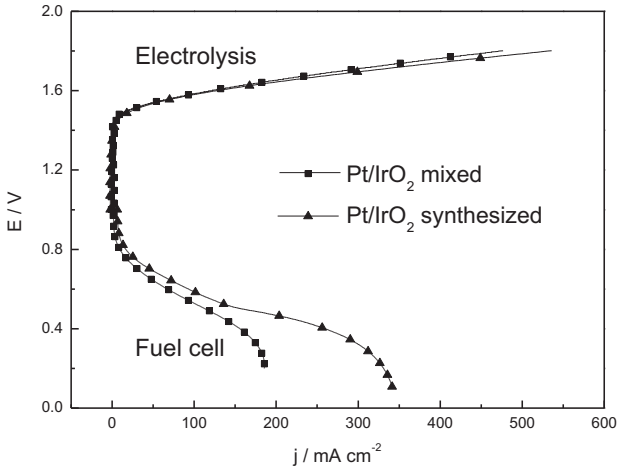

Fig. 9 – URFC polarization curves at room temperature of the MEAs based on synthesized and mixed Pt-IrO_2 (50:50 wt.%) electrocatalysts.

may be sufficient for URFC operation with renewable power sources [4].

The round-trip energy conversion efficiencies (ε_{RT}) during water electrolysis and fuel cell operation was calculated from the following equation [14,23,64]:

$$\varepsilon_{RT} = \frac{E_{FC}}{E_{WE}} \quad (1)$$

at different current densities. E_{FC} and E_{WE} are the cell voltages of the fuel cell and water electrolyzer, respectively, at a given current density. The values of round-trip energy efficiency for the cell based on the catalyst synthesized by this ultrasonic polyol method were about 47%, 37% and 30% at 50, 100 and 200 mA cm^{-2}, respectively. Most of the efficiency loss is due to the fuel cell mode which is strongly affected by the presence of Ti-backing layer, which causes the occurrence of electrode flooding already at low current densities as observed from the presence of a strong mass transport control. The latter is clearly envisaged from the limiting current. Probably, the presence of a hydrophilic Ti-backing layer for the oxygen electrode is more advantageous for the oxygen evolution than the oxygen reduction; the increase of overpotential as a function of current is much lower for the oxygen evolution process than the oxygen reduction. This conjecture was confirmed by an experiment carried out under fuel cell mode only, under the same operating conditions (RT, atmospheric pressure, dry gases) but using a commercial LT-ETEK carbon-based diffusion layer as the cathode catalyst backing layer instead of Ti grid. The modified configuration showed a peak power density of about 200 mW cm^{-2} (not shown); yet, neither carbon blacks nor carbon cloth/paper forming the conventional fuel cell backing layer are stable under the electrolyzer mode.

A proper tailoring of the oxygen electrode backing layer in terms of hydrophilic-hydrophobic properties may allow to compensate in part for this asymmetric behavior. Alternatively, an adjustment of the Pt/IrO_2 ratio in favor of a larger Pt content may provide a larger number of catalytic sites available for the oxygen reduction. This aspect will be addressed in a future work. However, from the stability point of view, it would not be appropriate to increase too much oxygen evolution overpotential in favor of a decrease of the overpotential for oxygen reduction. The stability of the oxygen reduction catalyst in fuel cells is primarily influenced by electrochemical potential, water content and temperature. A high operating potential plays the main role in determining the degradation of a conventional Pt/C cathode for fuel cells in terms of dissolution and sintering [16]. This process is promoted by the electrochemical corrosion of the carbon support conventionally used in fuel cell catalysts [65]. Typical accelerated degradation tests for the oxygen reduction electrocatalysts in fuel cells include potential holds at 1.2 V for 24 h or 1.4 V for 2 h. On the basis of such evidences, in order to carry out a stability test for the oxygen catalyst useful for both electrolysis and fuel cell mode, the system was tested for prolonged operation at a terminal voltage of 1.8 V. This represents the upper limit of the potential window for PEM electrolyzer operation under a suitable efficiency conditions (1.8 V corresponds to an efficiency of about 80% vs. the HHV of hydrogen), well above the potential window of a fuel cell cathode (0.6–1 V vs. RHE). Such a procedure is thus a stability test for the electrolyzer and an accelerated test for the fuel cell. It can be clearly observed in Fig. 10 that the electrolyzer performance is quite stable during 100 h operation at 1.8 V and the inset shows no significant change of the fuel cell polarization curve after this test. It is important to point out that a typical Pt/C fuel cell catalyst would be destroyed by such a degradation test as a consequence of carbon black oxidation to CO_2 at 1.8 V. This is not the case of the IrO_2-supported Pt electrocatalyst since the IrO_2 substrate is quite stable under such conditions possibly producing a further stabilization of Pt nanoparticles through a strong metal–support interaction (SMSI). Moreover, the formation of a passive Pt-oxide layer on the surface of Pt particles at such high potentials provides a barrier towards Pt dissolution.

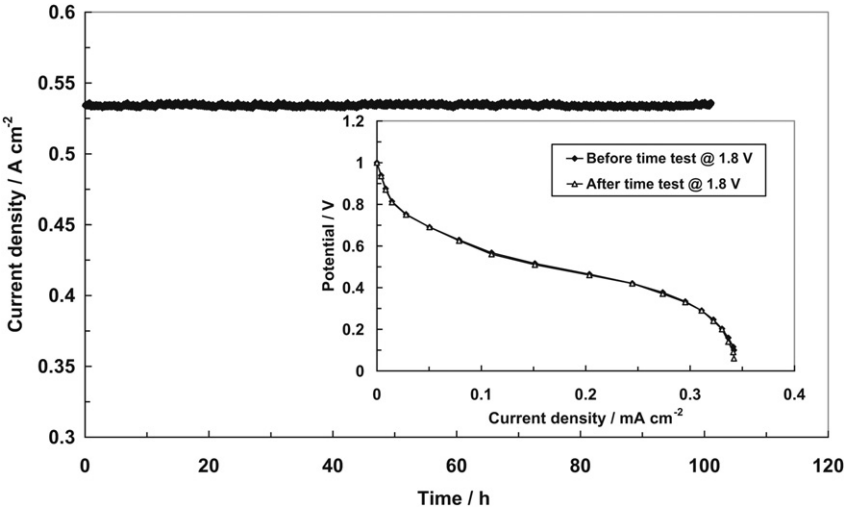

Fig. 10 – Time-stability test under electrolysis mode at 1.8 V and room temperature for the MEA based on Pt/IrO_2 (50:50 wt.%) electrocatalyst. The inset shows the fuel cell polarization curves before and after the stability test at room temperature.

4. Conclusions

The development of high energy density, efficient, non-polluting energy storage systems is fundamental for renewable power sources. A new process for synthesizing a nano-sized Pt/IrO_2 electrocatalyst for URFCs was developed. An advance with respect to the state of the art (mainly based on a mechanical mixing procedure) was achieved since a chemical deposition of Pt nanoparticles onto an IrO_2 support was obtained without modifying the oxidation state of Ir. Usually, the mechanical mixing of Pt and IrO_2 nanopowders is the most common approach to avoid modification of IrO_2 status. TEM observation showed an intimate contact between Pt and IrO_2 phases as required for a dual function catalyst operating in both electrolysis (oxygen evolution) and fuel cell (oxygen reduction) modes. Electrochemical data showed good performance at room temperature and atmospheric pressure, as required for operation in conjunction with renewable power sources, especially in the electrolyzer mode. To reduce the asymmetry of the overpotential for operation under electrolysis and fuel cell mode, it appears appropriate to tailor the catalyst composition as well as the hydrophilic/hydrophobic properties of the Ti-grid backing layer. However, to reduce the occurrence of corrosion phenomena, it is also necessary to avoid any increase of the maximum operating potential of the unitized regenerative fuel cell.

Acknowledgments

The authors acknowledge the support of bilateral CNR (Italy) – CONACYT (Mexico) joint agreement 2009–2011 (project Aricó/Arriaga Hurtado). J.C. Cruz and L.G. Arriaga thank the Mexican Council for Science and Technology (Conacyt, Fomix-Zacatecas 81728) for financial support. The efforts addressed by Tozzi Renewable Energy to this research topic are also acknowledged. CNR-ITAE authors acknowledge financial support from the FIRB MIUR Project “Rinnova”.

REFERENCES

[1] Aricò AS, Bruce P, Scrosati B, Tarascon JM, Van Schalkwijk W. Nanostructured materials for advanced energy conversion and storage devices. Nat Materials 2005;4:366–77.
[2] Shukla AK, Aricò AS, Antonucci V. An appraisal of electric automobile power sources. Renewable Sustainable Energy Rev 2001;5:137–55.
[3] Smith W. The role of fuel cells in energy storage. J Power Sources 2000;86:74–83.
[4] Barbir F. PEM electrolysis for production of hydrogen from renewable energy sources. Solar Energy 2005;78:661–9.
[5] Rasten E, Hagen G, Tunold R. Electrocatalysis in water electrolysis with solid polymer electrolyte. Electrochim Acta 2003;48:3945–52.
[6] de Oliveira-Sousa A, da Silva MAS, Machado SS, Avaca LA, de Lima-Neto P. Influence of the preparation method on the morphological and electrochemical properties of Ti/IrO_2-coated electrodes. Electrochim Acta 2000;45:4467–73.
[7] Mazumder V, Lee Y, Sun S. Recent development of active nanoparticle catalysts for fuel cell reactions. Adv Funct Mater 2010;20:1224–31.
[8] Gavello G, Zeng J, Francia C, Icardi UA, Graizzaro A, Specchia S. Experimental studies on Nafion® 112 single PEMFCs exposed to freezing conditions. Int J Hydrogen Energy 2011;36:8070–81.
[9] Kadirgan F, Kannan AM, Atilan T, Beyhan S, Ozenler SS, Suzer S, et al. Carbon supported nano-sized Pt-Pd and Pt-Co electrocatalysts for proton exchange membrane fuel cells. Int J Hydrogen Energy 2009;34:9450–60.
[10] Verma A, Basu S. Feasibility study of a simple unitized regenerative fuel cell. J Power Sources 2004;135:62–5.
[11] Grigoriev SA, Millet P, Porembsky VI, Fateev VN. Development and preliminary testing of a unitized regenerative fuel cell based on PEM technology. Int J Hydrogen Energy 2011;36:4164–8.
[12] Mitlitsky F, Myers B, Weisberg AH. Regenerative fuel cell systems. Energy & Fuels 1998;12:56–71.
[13] Dihrab SS, Sopian K, Alghoul MA, Sulaiman MY. Review of the membrane and bipolar plates materials for conventional and unitized regenerative fuel cells. Renewable Sustainable Energy Rev 2009;13:1663–8.
[14] Pettersson J, Ramsey B, Harrison D. A review of the latest developments in electrodes for unitised regenerative polymer electrolyte fuel cells. J Power Sources 2006;157:28–34.
[15] Liu C, Wang C-C, Kei C-C, Hsueh Y-C, Perng T- P. Atomic layer deposition of platinum nanoparticles on carbon nanotubes for application in proton-exchange membrane fuel cells. Small 2009;13:1535–8.
[16] Aricò AS, Stassi A, Modica E, Ornelas R, Gatto I, Passalacqua E, et al. Performance and degradation of high temperature polymer electrolyte fuel cell catalysts. J Power Sources 2008;178:525–36.
[17] Ioroi T, Oku T, Yasuda K, Kumagai N, Miyazaki Y. Influence of PTFE coating on gas diffusion backing for unitized regenerative polymer electrolyte fuel cells. J Power Sources 2003;124:385–9.
[18] Huang S-Y, Ganesan P, Jung H-Y, Popov BN. Development of supported bifunctional oxygen electrocatalysts and corrosion-resistant gas diffusion layer for unitized regenerative fuel cell applications. J Power Sources 2012;198:23–9.
[19] Chen G, Zhang H, Ma H, Zhong H. Effect of fabrication methods of bifunctional catalyst layers on unitized regenerative fuel cell performance. Electrochim Acta 2009;54:5454–62.
[20] Escalante-García IL, Duron-Torres SM, Cruz JC, Arriaga-Hurtado LG. Electrochemical characterization of IrO_2-Pt and RuO_2-Pt Mixtures as bifunctional electrodes for unitized regenerative fuel cells. J New Mat Electrochem Sys 2010;13:227–33.
[21] Zhang Y, Wang C, Wan N, Mao Z. Deposited RuO_2–IrO_2/Pt electrocatalyst for the regenerative fuel cell. Int J Hydrogen Energy 2007;32:400–4.
[22] Kiyosi K, Yoshito F. Sputter deposited Pt–Ir oxides thin films and their characterization. Mater SciEng B 2004;109:188–91.
[23] Jorissen L. Bifunctional oxygen/air electrodes. J Power Sources 2006;155:23–32.
[24] Grigoriev SA, Millet P, Dzhus KA, Middleton H, Saetre TO, Fateev VN. Design and characterization of bi-functional electrocatalytic layers for application in PEM unitized regenerative fuel cells. Int J Hydrogen Energy 2010;35:5070–6.
[25] Altmann S, Kaz T, Friedrich KA. Bifunctional electrodes for unitised regenerative fuel cells. Electrochim Acta 2011;56:4287–93.
[26] Antolini E, Salgado JRC, Giz MJ, Gonzalez ER. Effects of geometric and electronic factors on ORR activity of carbon

supported Pt-Co electrocatalysts in PEM fuel cells. Int J Hydrogen Energy 2005;30:1213–20.
[27] Yim S-D, Park G-G, Sohn Y-J, Lee W-Y, Yoon Y-G, Yang T-H, et al. Optimization of PtIr electrocatalyst for PEM URFC. Int J Hydrogen Energy 2005;30:1345–50.
[28] Sui S, Ma L, Zhai Y. TiC supported Pt–Ir electrocatalyst prepared by a plasma process for the oxygen electrode in unitized regenerative fuel cells. J Power Sources 2011;196: 5416–22.
[29] Chen GY, Delafuente DA, Sarangapani S, Mallouk TE. Combinatorial discovery of bifunctional oxygen reduction — water oxidation electrocatalysts for regenerative fuel cells. Catal Today 2001;67:341–55.
[30] Swette LL, Laconti AB, McCatty SA. Proton-exchange membrane regenerative fuel cells. J Power Sources 1994;47: 343–51.
[31] Swette LL, Kackley ND, Laconti AB. Regenerative fuel cells. 27th intersoc energy convers eng conf; 1992. 1101–1106.
[32] Liu H, Yi BL, Hou M, Wu JF, Hou ZJ, Zhang HM. Composite electrode for unitized regenerative proton exchange membrane fuel cell with improved cycle life. Electrochem Solid State Lett 2004;7:A56–9.
[33] Ioroi T, Kitazawa N, Yasuda K, Yamamoto Y, Takenaka H. Iridium oxide/platinum electrocatalysts for unitized regenerative polymer electrolyte fuel cells. J Electrochem Soc 2000;147:2018–22.
[34] Yao W, Yang J, Wang J, Nuli Y. Chemical deposition of platinum nanoparticles on iridium oxide for oxygen electrode of unitized regenerative fuel cell. Electrochem Commun 2007;9:1029–34.
[35] Cisar A, Murphy O, Clarke E. US Patent 0068544, 2003.
[36] Adams R, Shriner RL. Platinum oxide as a catalyst in the reduction of organic compounds. III. Preparation and properties of the oxide of platinum obtained by the fusion of chloroplatinic acid with sodium nitrate. J Am Chem Soc 1923; 45:2171–9.
[37] Tian ZQ, Jiang SP, Liu Z, Li L. Polyelectrolyte-stabilized Pt nanoparticles as new electrocatalysts for low temperature fuel cells. Electrochem Commun 2007;9:1613–8.
[38] Mayousse E, Maillard F, Fouda-Onana F, Sicardy O, Guillet N. Synthesis and characterization of electrocatalysts for the oxygen evolution in PEM water electrolysis. Int J Hydrogen Energy 2011;7:10474–81.
[39] Rioux RM, Song H, Grass M, Habas S, Niesz K, Hoefelmeyer JD. Monodisperse platinum nanoparticles of well-defined shape: synthesis, characterization, catalytic properties and future prospects. Top Catal 2006;39: 167–74.
[40] Jung H-Y, Park S, Popov BN. Electrochemical studies of an unsupported PtIr electrocatalyst as a bifunctional oxygen electrode in a unitized regenerative fuel cell. J Power Sources 2009;191:357–61.
[41] Hyung-Suk O, Jong-Gil O, Youn-Gi H, Hansung K. Investigation of carbon-supported Pt nanocatalyst preparation by the polyol process for fuel cell applications. Electrochim Acta 2007;52:7278–85.
[42] Watanabe M, Uchida M, Motoo S. Preparation of highly dispersed Pt+Ru alloy clusters and the activity for the electrooxidation of methanol. J Electroanal Chem 1987;229: 395–406.
[43] Masaharu T, Masayuki H, Yuki N. Synthesis of gold nanorods and nanowires by a microwave–polyol method. Mater Lett 2004;58:2326–30.
[44] Zhu YJ, Hu XL. Preparation of powders of selenium nanorods and nanowires by microwave-polyol method. Mater Lett 2004;58:1234–6.
[45] Gasteiger HA, Kocha SS, Sompalli B, Wagner FT. Activity benchmarks and requirements for Pt, Pt-alloy, and non-Pt oxygen reduction catalysts for PEMFCs. Appl Catal B Environ 2005;56:9–35.
[46] Bock C, Paquet C, Couillard M, Botton GA, MacDougall BR. Size-Selected synthesis of PtRu nano-catalysts: reaction and size control mechanism. J Am Chem Soc 2004;126: 8028–37.
[47] Antolini E. An empirical model to evaluate the contribution of alloyed and non-alloyed tin to the ethanol oxidation reaction on Pt-Sn/C catalysts based on the presence of SnO_2 and a Pt(1-x)Snx solid solution: application to DEFC performance. Int J Hydrogen Energy 2011;36:11043–7.
[48] Siracusano S, Baglio V, Stassi A, Ornelas R, Antonucci V, Aricò AS. Investigation of IrO_2 electrocatalysts prepared by a sulfite-couplex route for the O_2 evolution reaction in solid polymer electrolyte water electrolyzers. Int J Hydrogen Energy 2011;36:7822–31.
[49] Siracusano S, Baglio V, Di Blasi A, Briguglio N, Stassi A, Ornelas R, et al. Electrochemical characterization of single cell and short stack PEM electrolyzers based on a nanosized IrO_2 anode electrocatalyst. Int J Hydrogen Energy 2010;35: 5558–68.
[50] Cruz JC, Baglio V, Siracusano S, Ornelas R, Ortiz-Frade L, Arriaga LG, et al. Nanosized IrO_2 electrocatalysts for oxygen evolution reaction in an SPE electrolyzer. J Nanopart Res 2011;13:1639–46.
[51] Esmaeilifar A, Rowshanzamir S, Eikani MH, Ghazanfari E. Synthesis methods of low-Pt-loading electrocatalysts for proton exchange membrane fuel cell systems. Energy 2010; 35:3941–57.
[52] Lin KN, Liou WJ, Yang TY, Lin HM, Lin CK, Chien SH, et al. Synthesis of Hybrid Pt/TiO_2 (Anatase)/MWCNTs Nanomaterials by a combined sol-gel and polyol process. Diamond Relat Materials 2009;18:312–5.
[53] Chen W, Zhao J, Lee JY, Liu Z. Microwave heated polyol synthesis of carbon nanotubes supported Pt nanoparticles for methanol electrooxidation. Mat Chem Phys 2005;91: 124–9.
[54] Zhou Z, Zhou W, Wang S, Wang G, Jiang L, Li H, et al. Preparation of highly active 40 wt.% Pt/C cathode electrocatalysts for DMFC via different routes. Catal Today 2004;93:523–8.
[55] Zhao J, Chen W, Zheng Y, Li X, Xu Z. Microwave polyol synthesis of Pt/C catalysts with size-controlled Pt particles for methanol electrocatalytic oxidation. J Mat Sci 2006;41: 5514–8.
[56] Cruz JC, Baglio V, Siracusano S, Antonucci V, Aricò AS, Ornelas R, et al. Preparation and characterization of RuO_2 catalysts for oxygen evolution in a solid polymer electrolyte. Int J Electrochem Sci 2011;6:6607–19.
[57] Baglio V, Di Blasi A, Denaro T, Antonucci V, Aricò AS, Ornelas R, et al. Synthesis, characterization and evaluation of IrO_2-RuO_2 electrocatalytic powders for oxygen evolution reaction. J New Mat Electrochem Sys 2008;11:105–8.
[58] Di Blasi A, D'Urso C, Baglio V, Antonucci V, Aricò AS, Ornelas R, et al. Preparation and evaluation of RuO_2-IrO_2, IrO_2-Pt and IrO_2-Ta_2O_5 catalysts for the oxygen evolution reaction in an SPE electrolyzer. J Appl Electrochem 2009;39:191–6.
[59] Antonucci V, Di Blasi A, Baglio V, Ornelas R, Matteucci F, Ledesma Garcia J, et al. High temperature operation of a composite membrane-based solid polymer electrolyte water electrolyser. Electrochim Acta 2008;53:7350–6.
[60] Aricò AS, Shukla AK, Kim H, Park S, Min M, Antonucci V. An XPS study on oxidation states of Pt and its alloys with Co and Cr and its relevance to electroreduction of oxygen. Appl Surf Sci 2001;172:33–40.
[61] Moulder JF, Stickle WF, Sobol PE, Bomben KD. Handbook of X-ray photoelectron spectroscopy. Phys Electronics Inc; 1995.

[62] Antelman MS. The encyclopedia of chemical electrode potentials. New York: Plenum Press; 1982.
[63] Sunde S, Lervik IA, Tsypkin M, Owe L- E. Impedance analysis of nanostructured iridium oxide electrocatalysts. Electrochim Acta 2010;55:7751–60.
[64] Singh RN, Mishra D, Anindita A, Sinha ASK, Singh A. Novel electrocatalysts for generating oxygen from alkaline water electrolysis. Electrochem Commun 2007;9: 1369–73.
[65] Aricò AS, Stassi A, Gatto I, Monforte G, Passalacqua E, Antonucci V. Surface properties of Pt and PtCo electrocatalysts and their influence on the performance and degradation of high-temperature polymer electrolyte fuel cells. J Phys Chem C 2010;114:15823–36.